



Since January 2020 Elsevier has created a COVID-19 resource centre with free information in English and Mandarin on the novel coronavirus COVID-19. The COVID-19 resource centre is hosted on Elsevier Connect, the company's public news and information website.

Elsevier hereby grants permission to make all its COVID-19-related research that is available on the COVID-19 resource centre - including this research content - immediately available in PubMed Central and other publicly funded repositories, such as the WHO COVID database with rights for unrestricted research re-use and analyses in any form or by any means with acknowledgement of the original source. These permissions are granted for free by Elsevier for as long as the COVID-19 resource centre remains active.



## *In silico* drug discovery of major metabolites from spices as SARS-CoV-2 main protease inhibitors

Mahmoud A.A. Ibrahim<sup>a,\*</sup>, Alaa H.M. Abdelrahman<sup>a</sup>, Taha A. Hussien<sup>b</sup>, Esraa A.A. Badr<sup>a</sup>,  
Tarik A. Mohamed<sup>c</sup>, Hesham R. El-Seedi<sup>d,e</sup>, Paul W. Pare<sup>f</sup>, Thomas Efferth<sup>g</sup>,  
Mohamed-Elamir F. Hegazy<sup>c,g,\*\*</sup>

<sup>a</sup> Computational Chemistry Laboratory, Chemistry Department, Faculty of Science, Minia University, Minia, 61519, Egypt

<sup>b</sup> Pharmacognosy Department, Faculty of Pharmacy, Deraya University, Minia, Egypt

<sup>c</sup> Chemistry of Medicinal Plants Department, National Research Centre, 33 El-Bohouth St., Dokki, Giza, 12622, Egypt

<sup>d</sup> Department of Molecular Biosciences, The Wenner-Gren Institute, Stockholm University, S-106 91, Stockholm, Sweden

<sup>e</sup> International Research Center for Food Nutrition and Safety, Jiangsu University, Zhenjiang, 212013, China

<sup>f</sup> Department of Chemistry & Biochemistry Texas Tech University, Lubbock, TX, 79409 USA

<sup>g</sup> Department of Pharmaceutical Biology, Institute of Pharmaceutical and Biomedical Sciences, Johannes Gutenberg University, Staudinger Weg 5, 55128, Mainz, Germany

### ARTICLE INFO

#### Keywords:

Spices  
Secondary metabolites  
SARS-CoV-2 main protease  
Molecular dynamics  
Molecular docking

### ABSTRACT

Coronavirus Disease 2019 (COVID-19) is an infectious illness caused by Severe Acute Respiratory Syndrome Coronavirus 2 (SARS-CoV-2), originally identified in Wuhan, China (December 2019) and has since expanded into a pandemic. Here, we investigate metabolites present in several common spices as possible inhibitors of COVID-19. Specifically, 32 compounds isolated from 14 cooking seasonings were examined as inhibitors for SARS-CoV-2 main protease (M<sup>Pro</sup>), which is required for viral multiplication. Using a drug discovery approach to identify possible antiviral leads, *in silico* molecular docking studies were performed. Docking calculations revealed a high potency of salvianolic acid A and curcumin as M<sup>Pro</sup> inhibitors with binding energies of  $-9.7$  and  $-9.2$  kcal/mol, respectively. Binding mode analysis demonstrated the ability of salvianolic acid A and curcumin to form nine and six hydrogen bonds, respectively with amino acids proximal to M<sup>Pro</sup>'s active site. Stabilities and binding affinities of the two identified natural spices were calculated over 40 ns molecular dynamics simulations and compared to an antiviral protease inhibitor (lopinavir). Molecular mechanics-generalized Born surface area energy calculations revealed greater salvianolic acid A affinity for the enzyme over curcumin and lopinavir with energies of  $-44.8$ ,  $-34.2$  and  $-34.8$  kcal/mol, respectively. Using a STRING database, protein-protein interactions were identified for salvianolic acid A included the biochemical signaling genes ACE, MAPK14 and ESR1; and for curcumin, EGFR and TNF. This study establishes salvianolic acid A as an *in silico* natural product inhibitor against the SARS-CoV-2 main protease and provides a promising inhibitor lead for *in vitro* enzyme testing.

### 1. Introduction

Coronaviruses belong to the Coronaviridae family and are named for distinctive protein spikes covering the virus' outer membrane surface. Several members of the family are known to cause respiratory tract infections in humans ranging from mild common colds to severe SARS and MERS infections [1,2]. Coronavirus Disease 2019 (COVID-19) was first observed in Wuhan Province and identified by the Chinese Center for

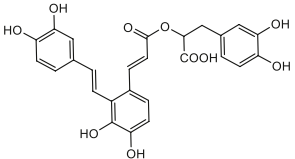
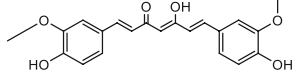
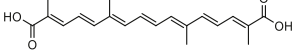
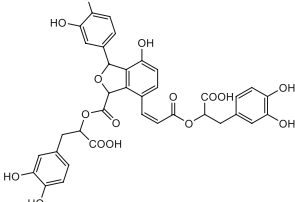
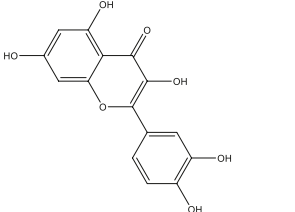
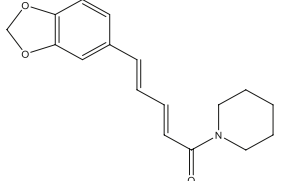
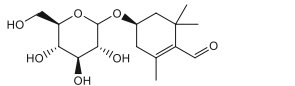
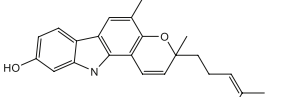
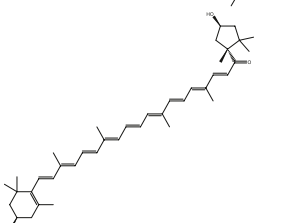
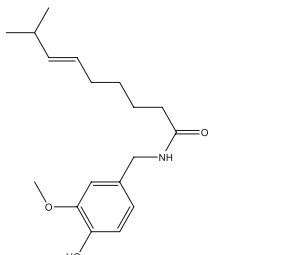

Disease Control and Prevention as Severe Acute Respiratory Syndrome Coronavirus 2 (SARS-CoV-2) [3,4]. The viral genome harbors 11 genes encoding 29 proteins and peptides; ([www.ncbi.nlm.nih.gov/nucore/NC\\_045512.2?report=graph](http://www.ncbi.nlm.nih.gov/nucore/NC_045512.2?report=graph)). Four proteins constitute the viral structure, including the spike or S protein [5]. In SARS-CoV-2, the S protein binds to an angiotensin-converting enzyme 2 (ACE2), a necessary step for viral entry into the host cell. Studies thus far indicate that the virus' S protein binds stronger to ACE2 than the one of SARS-CoV, providing a

\* Corresponding author. Computational Chemistry Laboratory, Chemistry Department, Faculty of Science, Minia University, Minia, 61519, Egypt.

\*\* Corresponding author. Chemistry of Medicinal Plants Department, National Research Centre, 33 El-Bohouth St., Dokki, Giza, 12622, Egypt.

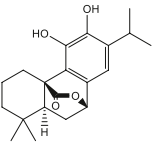
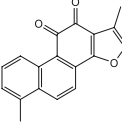
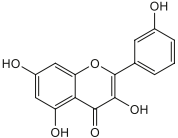
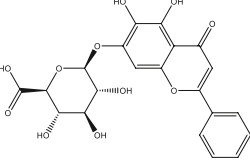
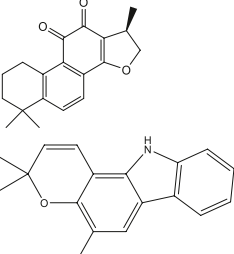
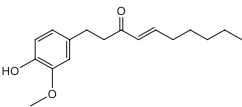
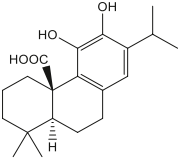
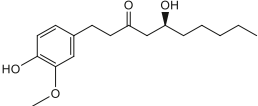
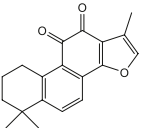
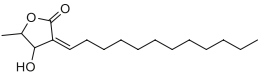
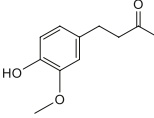
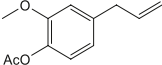

E-mail addresses: [m.ibrahim@compchem.net](mailto:m.ibrahim@compchem.net) (M.A.A. Ibrahim), [me.fathy@nrc.sci.eg](mailto:me.fathy@nrc.sci.eg) (M.-E.F. Hegazy).

**Table 1**  
Chemical structures, plant sources, docking scores, and binding features for 32 natural spices against SARS-CoV-2 main protease (M<sup>PRO</sup>).

Compound Name	Chemical Structure	Plant Source	Docking Score (kcal/mol)	Binding Features <sup>a</sup>
Salvianolic acid A		<i>Salvia officinalis</i> (Sage)	-9.7	GLU166 (2.24, 2.15 Å), PHE140 (2.09, 2.21 Å), GLN189 (2.74, 2.06 Å), TYR54 (3.01 Å), THR190 (1.87, 1.86 Å)
Curcumin		<i>Curcuma longa</i> (Turmeric)	-9.2	HIS163 (1.90 Å), CYS145 (2.72 Å), GLY143 (2.85 Å), SER144 (1.97, 2.01 Å), LEU141 (1.94 Å)
Crocetin		<i>Crocus sativus</i> (Saffron)	-8.9	ASP189 (1.84 Å), TYR54 (2.10 Å), CYS44 (1.79 Å), GLU166 (1.73 Å)
Salvianolic acid B		<i>Salvia officinalis</i> (Sage)	-8.5	GLU166 (2.87, 2.33 Å), THR190 (2.27, 1.93, 1.81 Å), MET49 (2.38 Å), HIS41 (2.05 Å), GLY143 (2.67 Å)
Quercetin		<i>Crocus sativus</i> (Saffron)	-8.3	THR190 (1.82 Å), GLU166 (2.07, 2.18 Å), ASP187 (2.05 Å)
Piperine		<i>Piper nigrum</i> (Black pepper)	-8.2	GLN189 (3.07 Å), GLY143 (2.15 Å)
Picrocrocin		<i>Crocus sativus</i> (Saffron)	-8.2	CYS145 (2.48 Å), GLU166 (2.56 Å), SER144 (3.09 Å), LEU141 (2.78, 2.17 Å), SER144 (2.19 Å)
Mahanine		<i>Murraya koenigii</i> (Curry leaf)	-8.0	MET165 (2.51 Å), THR190 (1.83 Å)
Capsanthin		<i>Capsicum annum</i> (Sweet pepper)	-8.0	TYR26 (2.60 Å), SER144 (2.79 Å), CYS145 (1.88 Å)
Capsaicin		<i>Capsicum annum</i> (Chili pepper)	-8.0	THR190 (2.25 Å), GLU166 (2.10, 2.10 Å)
Carnosol		<i>Rosmarinus officinalis</i> (Rosemary)	-7.9	GLU166 (2.21 Å)

(continued on next page)

Table 1 (continued)

Compound Name	Chemical Structure	Plant Source	Docking Score (kcal/mol)	Binding Features <sup>a</sup>
Tanshinone I		<i>Salvia officinalis</i> (Sage)	-7.8	GLU166 (1.95 Å)
Kaempferol		<i>Crocus sativus</i> (Saffron)	-7.8	THR190 (1.96 Å), ASP187 (1.95 Å), HIS164 (2.22 Å)
Baicalin		<i>Rosmarinus officinalis</i> (Rosemary)	-7.6	ASN142 (2.54 Å), GLY143 (2.14 Å), HIS163 (2.10 Å)
Cryptotanshinone		<i>Salvia officinalis</i> (Sage)	-7.6	GLU166 (1.92 Å)
Girinimbine		<i>Murraya koenigii</i> (Curry leaf)	-7.5	MET165 (2.80 Å), ARG188 (2.10 Å)
Shogaols		<i>Zingiber officinale</i> (Ginger)	-7.4	THR190 (2.27 Å), GLU166 (2.01 Å)
Carnosic acid		<i>Rosmarinus officinalis</i> (Rosemary)	-7.3	GLN189 (2.18 Å)
Gingerols		<i>Zingiber officinale</i> (Ginger)	-7.1	THR190 (2.21 Å), GLU166 (2.01 Å), HIS164 (1.80 Å)
Tanshinone IIA		<i>Salvia officinalis</i> (Sage)	-6.7	— <sup>b</sup>
Marliolide		<i>Cinnamomum verum</i> (Cinnamon)	-6.2	THR190 (2.03 Å)
Zingerone		<i>Zingiber officinale</i> (Ginger)	-5.7	CYS44 (2.74 Å), GLU166 (2.18 Å)
Acetylugenol		<i>Zingiber officinale</i> (Ginger)	-5.3	CYS145 (1.95 Å)
Thymoquinone		<i>Nigella sativa</i> (Black seeds)	-5.2	— <sup>b</sup>

(continued on next page)

Table 1 (continued)

Compound Name	Chemical Structure	Plant Source	Docking Score (kcal/mol)	Binding Features <sup>a</sup>
Safranal		<i>Crocus sativus</i> (Saffron)	-5.2	— <sup>b</sup>
Eugenol		<i>Syzygium aromaticum</i> (Cloves)	-5.1	GLU166 (1.99 Å)
S-Allyl cysteine		<i>Allium sativum</i> (Garlic) and/or <i>Allium cepa</i> (Onion)	-4.4	ARG188 (2.14 Å), THR190 (1.92 Å), GLN192 (2.34 Å), GLU166 (1.85)
Di-allyl trisulfide		<i>Allium sativum</i> (Garlic) and/or <i>Allium cepa</i> (Onion)	-4.1	— <sup>b</sup>
Dipropyl disulfide		<i>Allium sativum</i> (Garlic) and/or <i>Allium cepa</i> (Onion)	-3.7	— <sup>b</sup>
Di-allyl disulfide		<i>Allium sativum</i> (Garlic) and/or <i>Allium cepa</i> (Onion)	-3.7	— <sup>b</sup>
Dipropyl sulfide		<i>Allium sativum</i> (Garlic) and/or <i>Allium cepa</i> (Onion)	-3.6	— <sup>b</sup>
Di-allyl sulfide		<i>Allium sativum</i> (Garlic) and/or <i>Allium cepa</i> (Onion)	-3.5	— <sup>b</sup>

<sup>a</sup> Conventional hydrogen bond only is listed. For the other interactions, see Fig. S1.

<sup>b</sup> No hydrogen bond was observed.

rationale why COVID-19 so easily spreads and is highly infectious. Another group of SARS-CoV-2 proteins controls how the virus replicates as well as avoids the host's immune system. These non-structural proteins initially expressed as two large polyproteins are processed into 16 peptide components. The main protease ( $M^{pro}$  or 3CLpro), cleaves the polyproteins into 11 fragments, whose structures were recently elucidated and an inhibitor that blocks the  $M^{pro}$  catalytic activity identified [6]. From this work,  $M^{pro}$  appears to be a promising target for designing small molecule inhibitors.

COVID-19 rapidly spreads due to the global mobility of humans and is currently present in more than 200 countries. Patients mainly suffer from fever, dry cough, labored breathing, and bilateral lung infiltrates. The causative agent is diagnosed from throat or nasal swabs with nucleic acid sequence similarity. Rapid disease spreading coupled with high mortality rates makes COVID-19 a major global public health threat [7]. Recently, emergency use of remdesivir has been issued by the U.S. Food and Drug Administration for treatment of COVID-19. With few treatment options available, there is an urgent need to seek out effective strategies for prophylaxis for such viral outbreaks. Using experimental methods of drug discovery is time-consuming and costly. Therefore, structure-based computational modeling of ligand-receptor interactions can be used to identify potential  $M^{pro}$  inhibitors to block viral replication.

Herbal extracts and spices are natural immune boosters and/or anti-infective agents currently utilized in many parts of the world [8]. In traditional folk medicine, spices, botanical detoxifiers [9], antioxidants [10] and plant haematinics [11] are used as antiviral mediators to prevent/minimize disease. Low toxicity makes such metabolites well suited as drug leads for viral diseases such as COVID-19. In this study, selected spices with documented, biologically activity (e.g. cinnamon, clove, ginger, mustard and others) were exemplarily chosen to generate

a metabolite library for the screening of  $M^{pro}$ -specific drug candidates with presumable effectiveness against COVID-19.

## 2. Materials and methods

### 2.1. $M^{pro}$ preparation

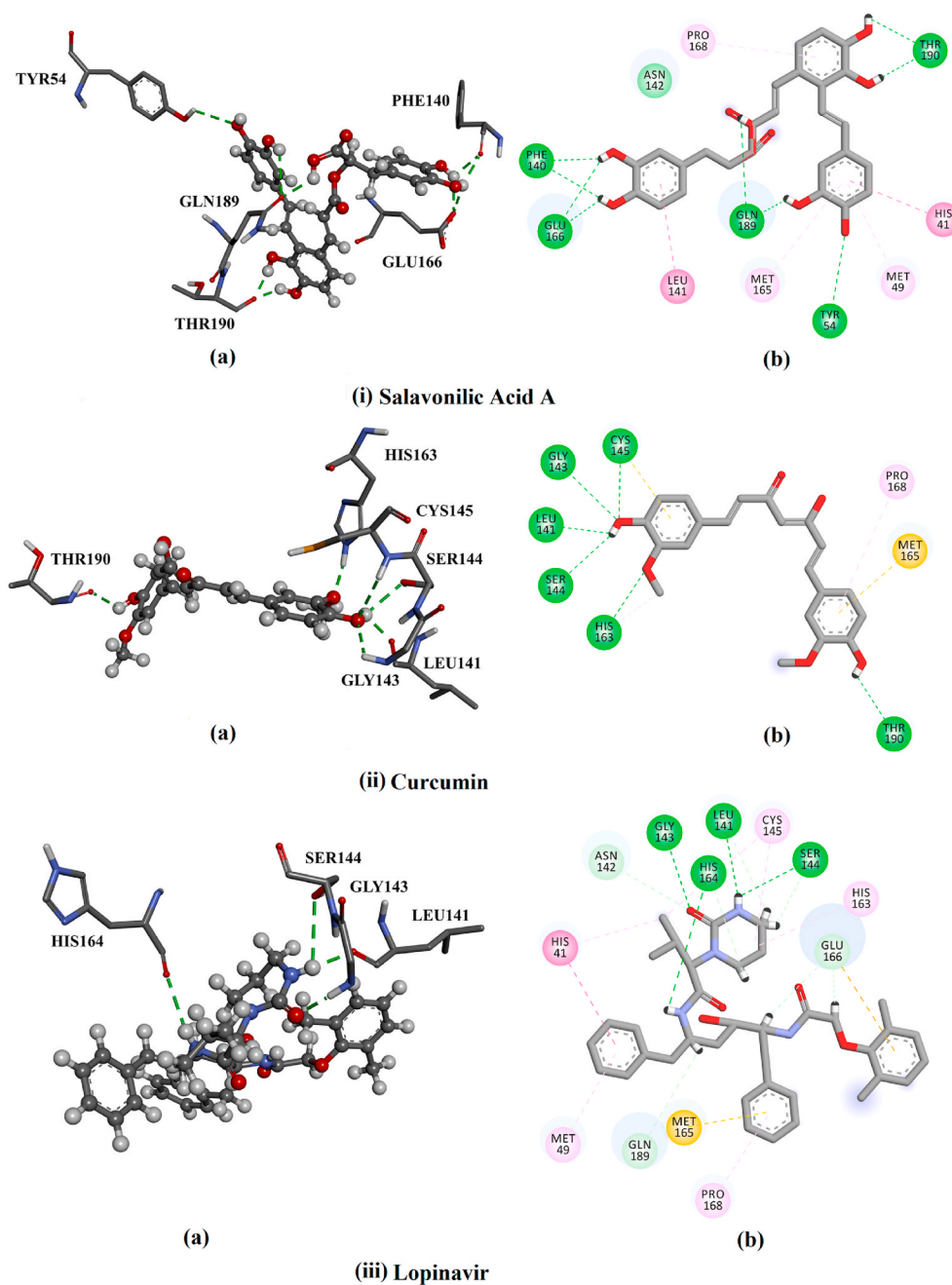
The resolved crystal structure of the main protease ( $M^{pro}$ ) of SARS-CoV-2 in complex with N3 inhibitor (PDB code: 6LU7 [12]) was used for molecular docking as well as molecular dynamics calculations. Water and spectator ions were deleted. H++ server was used to study the protonation state of  $M^{pro}$  and to add all missing hydrogen atoms [13]. In H++ calculations, the following physical conditions were applied: pH = 6.5, internal dielectric = 10, external dielectric = 80 and salinity = 0.15.

### 2.2. Inhibitor preparation

The chemical structures of the 32 investigated natural spices were retrieved from the PubChem database and their 3D structures were generated using Omega2 software [14,15]. All generated structures were minimized using Merck Molecular Force Field 94 (MMFF94S) with the assistance of available software (SZYBKI) [16]. The 2D chemical structures of the investigated compounds are illustrated in Table 1.

### 2.3. Molecular docking

For molecular docking calculations, AutoDock4.2.6 software was utilized [17]. The pdbqt file of SARS-CoV-2  $M^{pro}$  was prepared according to the AutoDock protocol [18]. In AutoDock4.2.6, default parameters were employed, except the numbers of genetic algorithm (GA) run and energy evaluations (eval). GA and eval were set to 250 and 25, 000, 000,



### Interactions

<span style="color: green;">■</span> van der Waals	<span style="color: magenta;">■</span> Amide-Pi Stacked	<span style="color: lightpink;">■</span> Alkyl
<span style="color: cyan;">■</span> Carbon Hydrogen Bond	<span style="color: pink;">■</span> Pi-Pi T-shaped	<span style="color: lightpurple;">■</span> Pi-Alkyl
<span style="color: green;">■</span> Conventional Hydrogen Bond	<span style="color: red;">■</span> Unfavorable Donor-Donor	<span style="color: yellow;">■</span> Pi-Sulfur

**Fig. 1.** (a) 3D and (b) 2D representations of interactions of (i) salvanolic acid A, (ii) curcumin and (iii) lopinavir with amino acid residues of SARS-CoV-2 main protease ( $M^{pro}$ ).

respectively. The grid was defined to cover the active site of the SARS-CoV-2  $M^{pro}$ . The grid size and spacing value were  $60 \text{ \AA} \times 60 \text{ \AA} \times 60 \text{ \AA}$  and  $0.375 \text{ \AA}$ , respectively. The grid center coordinates were  $-13.069, 9.740, 68.490$  (XYZ assignments, respectively). The atomic charges of studied natural spices were assigned using the Gasteiger method [19]. The predicted binding poses for each compound were processed by the built-in clustering analysis ( $1.0 \text{ \AA}$  RMSD tolerance), with the conformation of the lowest energy with respect to the largest cluster selected as representative.

### 2.4. Molecular dynamics simulations

AMBER16 software was utilized to conduct molecular dynamics (MD) simulation for the natural spices in complex with SARS-CoV-2  $M^{pro}$  [20]. The details of the employed MD simulations are described in Ref. [21,22]. In brief, general AMBER force field (GAFF) [23] and AMBER force field 14SB [24] were applied to describe spices compounds and  $M^{pro}$ , respectively. Restrained electrostatic potential (RESP) approach [25] was utilized to assign the atomic partial charges of the



**Table 2**

Calculated average MM-GBSA binding energies and the corresponding energy components for lopinavir and the two identified potent natural spices components in complex with SARS-CoV-2 main protease (M<sup>Pro</sup>) over 40 ns MD simulations.

Compound Name	Calculated MM-GBSA binding energy (kcal/mol)						
	$\Delta E_{VDW}$	$\Delta E_{ele}$	$\Delta E_{GB}$	$\Delta E_{SUR}$	$\Delta G_{gas}$	$\Delta G_{solv}$	$\Delta G_{binding}$
Salvianolic acid A	-45.4	-65.5	72.5	-6.3	-111.0	66.1	-44.8
Curcumin	-47.5	-19.8	39.2	-6.1	-67.4	33.1	-34.2
Lopinavir	-46.8	-26.1	43.9	-5.9	-72.8	38.0	-34.8

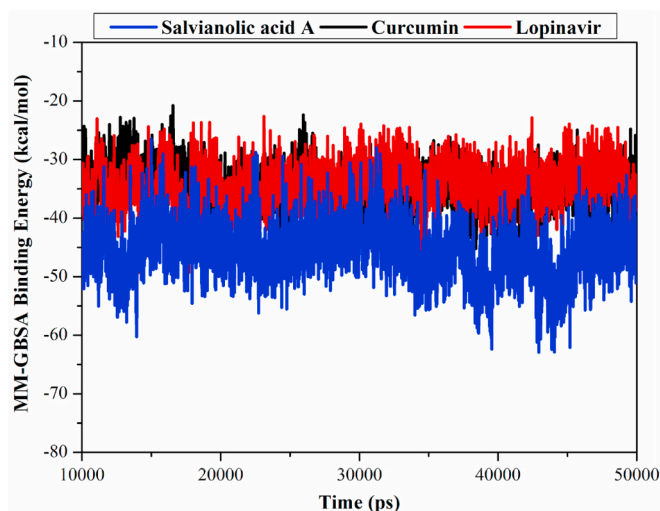


**Fig. 2.** Estimated MM-GBSA binding energies (in kcal/mol) for salvianolic acid A, curcumin and lopinavir, with SARS-CoV-2 main protease (M<sup>Pro</sup>) during 40 ns MD simulation.

natural spices using Gaussian09 software [26]. Docked spice-M<sup>Pro</sup> complexes were water solvated with 15 Å distances between the box edge and atoms of the spice-M<sup>Pro</sup> complexes. Solvated spice-M<sup>Pro</sup> complexes were minimized by 5000 steps and afterward smoothly heated from 0 K to 300 K over a brief interval (50 ps). Using periodic boundary conditions and NPT ensemble, the spice-M<sup>Pro</sup> systems were simulated for 10 ns of equilibration and 40 ns of production. All molecular dynamics simulations were carried out with pmemd.cuda implemented in AMBER16. All molecular docking and molecular dynamics calculations were performed on CompChem GPU/CPU cluster ([hpc.compchem.net](http://hpc.compchem.net)).

## 2.5. MM-GBSA binding energy

The binding energies of the investigated spices compounds with SARS-CoV-2 M<sup>Pro</sup> were estimated using molecular mechanical-generalized Born surface area (MM-GBSA) approach with modified GB model (igb = 2) implemented in AMBER16 software [27]. For the MM-GBSA calculations, uncorrelated snapshots were collected over the production run, and a single-trajectory approach was employed, in which compound, receptor, and complex coordinates were retrieved from a single trajectory. The binding energy ( $\Delta G_{binding}$ ) was estimated as follows:

$$\Delta G_{binding} = G_{Complex} - (G_{Compound} + G_{M^{Pro}})$$

where the energy term ( $G$ ) is estimated as:

$$G = E_{vdw} + E_{ele} + G_{GB} + G_{SA}$$

$E_{vdw}$  and  $E_{ele}$  are van der Waals and electrostatic energies, respectively. The electrostatic solvation free energy ( $G_{GB}$ ) was calculated from the generalized Born (GB) equation. The nonpolar energy ( $G_{SA}$ ) was estimated with the solvent-accessible surface area (SASA). For all investigated natural spices, entropy contributions were neglected.

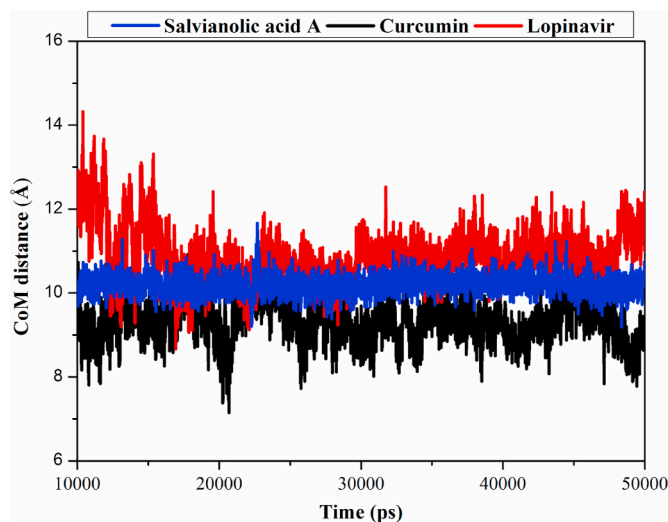


**Fig. 3.** Center-of-mass (CoM) distances (in Å) between salvianolic acid A, curcumin and lopinavir and GLY143 of SARS-CoV-2 main protease (M<sup>Pro</sup>) during 40 ns MD simulation.

## 2.6. Drug likeliness

The physicochemical parameters of the most promising natural spices as SARS-CoV-2 M<sup>Pro</sup> inhibitors were predicted using the online Molinspiration cheminformatics software (<http://www.molinspiration.com>). The predicted parameters included the number of rotatable bonds (nrotb), number of hydrogen bond acceptors (nON), number of hydrogen bond donors (nOHNH), *n*-octanol/water partition coefficient (P), molecular weight (MWt), molecular volume (MVol), topological polar surface area (TPSA) and percent absorption (% ABS). %ABS was estimated as follows [28]:

$$\%ABS = 109 - [0.345 \times TPSA]$$

## 2.7. Protein-protein interaction

The online web-based tools of SwissTargetPrediction (<http://www.swisstargetprediction.ch>) were applied to predict the biological targets for the most promising natural spices as SARS-CoV-2 M<sup>Pro</sup> inhibitors. The DisGeNET online database (<https://www.disgenet.org>) was utilized to collect the available database for SARS diseases. Venn Diagram was designed using InteractiVenn online tool [29]. Protein-protein interaction (PPI) network was generated using a STRING functional database for top predicted targets [30]. Cytoscape 3.8.0 was employed to investigate target-function relation based on the network topology [31].

## 3. Results and discussion

Lack of treatments against COVID-19 pinpoints a critical need to systematically screen and identify compounds that can block viral

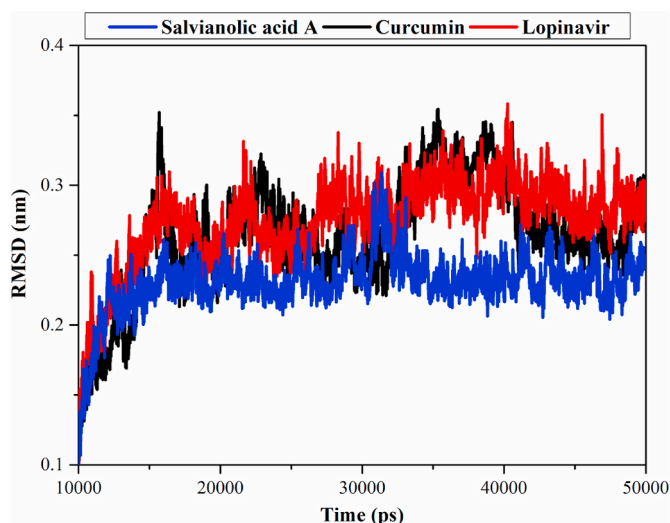


Fig. 4. Root-mean-square deviation (RMSD) of the backbone atoms from the initial structure for salvianolic acid A, curcumin, and lopinavir with the SARS-CoV-2 main protease ( $M^{pro}$ ) over 40 ns MD simulation.

reproduction. Since the main protease of SARS-CoV-2 ( $M^{pro}$ ) plays a critical role in the viral replication process, structure-based computational modeling of ligand-receptor interactions and molecular dynamics has been used to screen metabolites from common spices as potential  $M^{pro}$  inhibitors. Indeed several herbal plants have already been reported as antiviral entities against hepatitis B, respiratory syncytial virus and influenza [32].

### 3.1. Molecular docking

Molecular docking technique was utilized to predict binding modes and affinities of 32 natural products towards SARS-CoV-2  $M^{pro}$ . Compounds were prepared and docked into the virus  $M^{pro}$  active site using AutoDock4.2.6 software. Docking scores were estimated and the corresponding binding features were analyzed (Table 1). Most docked natural products shared the same binding modes, forming hydrogen bonds with key amino acid residues in the active site such as THR190, GLY143, CYS145, and GLU166. 2D binding modes for each of the compounds are displayed in Fig. S1. A wide range of docking scores was observed ranging from  $-3.5$  to  $-9.7$  kcal/mol. Salvianolic acid A, a phenolic acid obtained from sage (*Salvia officinalis*) showed the highest binding affinity towards SARS-CoV-2  $M^{pro}$  with a docking score of  $-9.7$  kcal/mol. Curcumin, phenolic compound separated from turmeric (*Curcuma longa*), exhibited the second highest binding affinity with a docking score of  $-9.2$  kcal/mol. The surpass potentialities of salvianolic acid A and curcumin as  $M^{pro}$  inhibitors are attributed to their ability to form multiple hydrogen bonds, van der Waals interactions as well as hydrophobic and pi-based interactions with the key amino acids within the active site (Fig. 1). Specifically, salvianolic acid A forms nine hydrogen bonds with GLU166, PHE140, GLN189, TYR54, and THR190 amino acid with bond lengths ranging from 1.86 to 3.01 Å (Fig. 1). Compared to salvianolic acid A, curcumin formed fewer hydrogen bonds with (six hydrogen bonds, interacting with HIS163, CYS145, GLY143, SER144 and LEU141 with bond lengths ranging from 1.90 to 2.85 Å, Fig. 1). In

contrast, some natural products were not capable of similar active site bonding such as tanshinone IIA, thymoquinone, safranal, diallyl trisulfide, dipropyl disulfide, diallyl disulfide, dipropyl sulfide and diallyl sulphide. Absence of such hydrogen bonding resulted in weak natural product- $M^{pro}$  binding affinity.

The peptidomimetic molecule lopinavir, which functions as an antiretroviral protease inhibitor against HIV was used as a positive control [33,34] as it has recently been clinically investigated as an anti-COVID-19 drug [35,36]. Lopinavir exhibited high binding affinity ( $-9.8$  kcal/mol) forming four hydrogen bonds with HIS164, SER144, LEU141, and GLY143 with bond lengths of 2.62, 3.09, 1.96 and 2.01 Å, respectively (Fig. 1). A docking comparison of lopinavir with salvianolic acid A and curcumin revealed competing binding affinities suggesting the *in silico* potentiality of the three compounds as  $M^{pro}$  inhibitors.

### 3.2. MD simulation and binding energy calculations

Since the reliability of ligand-enzyme binding energies using molecular docking scores have been questioned due to complicating environmental factors such as a lack of ligand-receptor flexibility, solvent effects, and dynamics [37,38], molecular dynamics (MD) simulations are employed to increase the reliability of predicted ligand-enzyme binding energies. Salvianolic acid A and curcumin were further investigated by MD over 40 ns simulation time. Based on collected compound- $M^{pro}$  snapshots over the production stage of 40 ns, the binding energies ( $\Delta G_{binding}$ ) were estimated using MM-GBSA approach and summarized in Table 2. Salvianolic acid A and curcumin displayed robust binding affinities ( $\Delta G_{binding}$ ) with values of  $-44.8$  and  $-34.2$  kcal/mol, respectively. Compared with lopinavir ( $\Delta G_{binding} = -34.8$  kcal/mol), the MM-GBSA binding affinity of curcumin is similar to that of lopinavir, while salvianolic acid A, in fact, showed a significantly higher binding energy.

MM-GBSA binding energies were decomposed to identify the nature of the predominant interactions. The estimated energy components for salvianolic acid A-, curcumin- and lopinavir- $M^{pro}$  complexes are listed in Table 2. For salvianolic acid A, binding energy was dominated by  $E_{ele}$  interactions with an average value of  $-65.5$  kcal/mol which was three times higher than that of lopinavir and curcumin, with an average value of  $-26.1$  and  $-19.8$  kcal/mol, respectively. This is attributed to a higher number of hydrogen bonds for salvianolic acid A with the key amino acids inside  $M^{pro}$ 's active site, compared to lopinavir or curcumin (Table 1).  $E_{vwd}$  interactions were the dominant force in the binding affinity of lopinavir and curcumin with an average value of  $-46.8$  and  $-47.5$  kcal/mol, respectively while salvianolic acid had an average value of  $-45.4$  kcal/mol. Together these results provide quantitative data of the binding affinities of salvianolic acid A and curcumin as SARS-CoV-2  $M^{pro}$  inhibitors.

### 3.3. Post-MD analyses

While molecular docking and MD combined with MM-GBSA binding energy calculation revealed the potentiality of salvianolic acid A and curcumin as SARS-CoV-2  $M^{pro}$  inhibitors, additional MD-based analyses would be required to demonstrate structural and energetic stabilities for ligand-enzyme interactions. The structural and energetical analyses included binding energy per-frame, center-of-mass (CoM) distance, and root-mean-square deviation (RMSD).

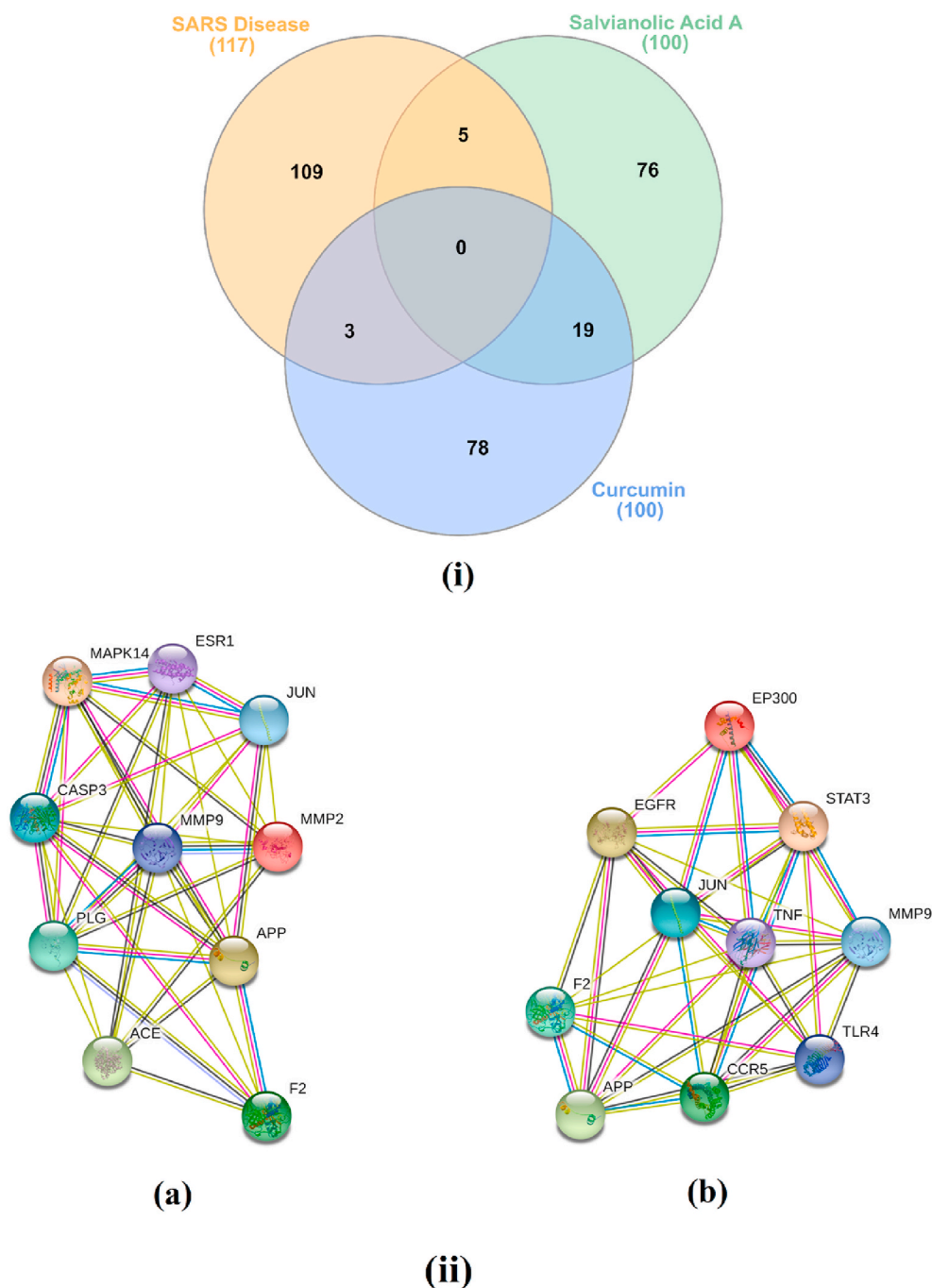
MM-GBSA binding energy per-frame for salvianolic acid A and

Table 3

Predicted physicochemical parameters of the two identified natural spices as putative SARS-CoV-2 main protease ( $M^{pro}$ ) inhibitors and their different structural descriptors.

Compound name	miLog P	TPSA	nON	nOHNH	Nrotb	MVol	MWt	%ABS
Salvianolic acid A	3.0	185	10	7	9	418	494	45%
Curcumin	2.9	116	7	4	7	323	370	69%





**Fig. 5.** (i) Venn diagram analysis for salvianolic acid A and curcumin and SARS disease genes, and (ii) STRING PPI network for the top 10 targets for (a) salvianolic acid A and (b) curcumin as potent SARS-CoV-2 main protease ( $M^{pro}$ ) inhibitors.

curcumin were evaluated and compared to lopinavir over 40 ns MD simulations (Fig. 2). As can be seen from data in Fig. 2, overall stabilities for salvianolic acid A- $M^{pro}$ , curcumin- $M^{pro}$ , and lopinavir- $M^{pro}$  complexes were observed throughout the MD simulation with average binding energies ( $\Delta G_{binding}$ ) of  $-44.8$ ,  $-34.2$  and  $-34.8$  kcal/mol, respectively. These results indicated satisfactory stabilities of the ligand-enzyme complexes.

Center-of-mass (CoM) distance between an inhibitor and an essential amino acid residue would give a deeper insight into the stability of ligand-enzyme complex over the MD simulation. Therefore, CoM distances between salvianolic acid A, curcumin and lopinavir and  $M^{pro}$  GLY143 were measured (Fig. 3). The CoM distances were more narrow-fluctuated for salvianolic acid A compared to curcumin or lopinavir

complexes, with average CoM distances of 10.7, 11.2 and 11.1 Å, respectively. These findings indicated that salvianolic acid A bounds more tightly with  $M^{pro}$  complex compared to curcumin and lopinavir.

Root-mean-square deviation (RMSD) for the complex backbone atoms was estimated to inspect the structural changes in the  $M^{pro}$ . For salvianolic acid A- $M^{pro}$  and lopinavir- $M^{pro}$  complexes, RMSD was observed to be below 0.25 nm while curcumin- $M^{pro}$  exhibited slightly lower stability (Fig. 4). Consistency of these energetic and structural measurements, salvianolic acid A is ranked as having higher complex stability than curcumin or lopinavir.

### 3.4. Drug-likeness

Drug-likeness is a qualitative measure utilized in drug discovery to evaluate pharmacokinetic properties such as oral bioavailability. Physicochemical parameters were evaluated using Molinspiration cheminformatics (<http://www.molinspiration.com>), online software calculation toolkit. The predicted parameters are summarized in Table 3. The permeability across the cell membrane, as measured by the  $\text{mlog P}$  value, was less than five (2.9 and 3.0 for salvianolic acid A and curcumin, respectively) indicating that these components have satisfactory membrane permeability. Moreover, their molecular weights of 494 and 370, for salvianolic acid A and curcumin, respectively, should be readily transferred, diffused and absorbed. Another parameter indicating of molecular bioabsorption is the topological polar surface area (TPSA) calculated as a surface sum of polar atoms or molecules, including oxygen, nitrogen and attached hydrogens. Molecules with a TPSA greater than 140 Å squared tend to be poor at permeating cell membranes, whereas a TPSA less than 90 Å squared is usually highly favorable. Salvianolic acid A and curcumin TPSAs of 185 and 116 Å, respectively, indicate an intermediate cell membrane permeability and oral bioavailability level.

### 3.5. Molecular target prediction and network analysis

Salvianolic acid A and curcumin protein targets were predicted and classified using a SwissTargetPrediction (Fig. S2). One hundred and seventeen genes were identified using DisGeNET online tools for Severe Acute Respiratory Syndrome diseases (SARS, C1175175). Utilizing Venn diagram comparison analysis, commonly shared genes for salvianolic acid A included ACE, CASP3, CASP1, ESR1 and MAPK14, and for curcumin TNF, EGFR and ADAM17 (Fig. 5). Angiotensin-converting enzyme 2 (ACE2) is a host protein and the receptor for SARS-CoV-2 entry [39]. MAPK14 inhibition is predicted to block the ACE2 signaling pathway, and in turn, reduce cell internalization of SARS-CoV-2. For SARS-S ADAM17-dependent shedding of ACE2, a process coupled with TNF- $\alpha$  production, reduced viral reproduction [40]. Salvianolic acid A and curcumin predicted genes targets were also analyzed via a STRING PPI network and visualized by Cytoscape 3.8.0. The top 10 scored genes for salvianolic acid A included ACE, MAPK14 and ESR1 and for curcumin EGFR and TNF (Table S1).

## 4. Conclusions

The COVID-19 pandemic has had a catastrophic impact on human health and global economies. SARS-CoV-2 main protease ( $M^{\text{pro}}$ ) may well prove to be the Achilles heel of viral replication. Using molecular docking and molecular dynamics approaches, 32 natural products were screened as possible competitive inhibitors of  $M^{\text{pro}}$ . Molecular docking calculations revealed the high binding affinities of salvianolic acid A and curcumin towards  $M^{\text{pro}}$  with docking scores of  $-9.7$  and  $-9.2$  kcal/mol, respectively. The two compounds when subjected to MD simulations demonstrated promising binding affinities with  $M^{\text{pro}}$  (calculated MM-GBSA binding energies of  $-44.8$  and  $-34.2$  kcal/mol). Post-dynamics analyses were consistent with ligand-enzyme affinity and stability. Physicochemical parameters also exhibited promising drug-likeness properties. The results of the current study reveal two promising natural products, salvianolic acid A and curcumin as potential inhibitors of  $M^{\text{pro}}$ . Due to the limitation of experimental test, further *in vitro* and/or *in vivo* investigation of the potent natural metabolites under study is highly recommended as a promising starting point for the development of natural drugs targeting SARS-CoV-2  $M^{\text{pro}}$ .

### Author contributions

Conceptualization, Mahmoud Ibrahim and Mohamed Elamir F. Hegazy; Data curation, Alaa Abdelrahman and Esraa Badr; Formal

analysis, Alaa Abdelrahman; Investigation, Alaa Abdelrahman and Mohamed Elamir F. Hegazy; Methodology, Mahmoud Ibrahim; Project administration, Mahmoud Ibrahim and Mohamed Elamir F. Hegazy; Resources, Mahmoud Ibrahim; Software, Mahmoud Ibrahim; Supervision, Mahmoud Ibrahim; Visualization, Alaa Abdelrahman; Writing – original draft, Alaa Abdelrahman, Taha Hussien, Esraa Badr and Tarik Mohamed; Writing – review & editing, Mahmoud Ibrahim, Hesham El-Seedi, Paul W. Paré, Thomas Efferth and Mohamed Elamir F. Hegazy. All authors have read and agreed to the published version of the manuscript.

### Funding

The computational work was completed with resources supported by the Science and Technology Development Fund, STDF, Egypt, Grants No. 5480 & 7972 (Granted to Mahmoud Ibrahim).

### Declaration of competing interest

The authors declare no conflict of interest.

### Acknowledgments

Prof. Mohamed Hegazy gratefully acknowledges the financial support from Alexander von Humboldt Foundation “Georg Foster Research Fellowship for Experienced Researchers”. Prof. Hesham.R. El-Seedi is very grateful to the Swedish Research Council VR (grants 2015–05468 and 2016–05885).

### Appendix A. Supplementary data

Supplementary data to this article can be found online at <https://doi.org/10.1016/j.compbmed.2020.104046>.

### References

- [1] P.C. Woo, Y. Huang, S.K. Lau, K.Y. Yuen, Coronavirus genomics and bioinformatics analysis, *Viruses* 2 (2010) 1804–1820.
- [2] Y. Yin, R.G. Wunderink, MERS, SARS and other coronaviruses as causes of pneumonia, *Respirology* 23 (2018) 130–137.
- [3] N. Zhu, D. Zhang, W. Wang, X. Li, B. Yang, J. Song, X. Zhao, B. Huang, W. Shi, R. Lu, P. Niu, F. Zhan, X. Ma, D. Wang, W. Xu, G. Wu, G.F. Gao, W. Tan, China novel coronavirus, T. Research, A novel coronavirus from patients with pneumonia in China, 2019, *N. Engl. J. Med.* 382 (2020) 727–733.
- [4] World Health Organization, WHO director-general’s remarks at the media briefing on 2019-nCoV on 11 February, 2020 [cited 2020 Apr 2], Available from: <https://www.who.int/dg/speeches/detail/who-director-general-s-remarks-at-the-media-briefing-on-2019-ncov-on-11-february-2020>, 2020.
- [5] Z. Liu, X. Xiao, X. Wei, J. Li, J. Yang, H. Tan, J. Zhu, Q. Zhang, J. Wu, L. Liu, Composition and divergence of coronavirus spike proteins and host ACE2 receptors predict potential intermediate hosts of SARS-CoV-2, *J. Med. Virol.* 92 (2020) 595–601.
- [6] L. Zhang, D. Lin, X. Sun, U. Curth, C. Drosten, L. Sauerhering, S. Becker, K. Rox, R. Hilgenfeld, Crystal structure of SARS-CoV-2 main protease provides a basis for design of improved alpha-ketoamide inhibitors, *Science* 368 (2020) 409–412.
- [7] (Live) Coronavirus Update, 2,418,429 cases and 165,739 deaths from COVID–19 virus pandemic—worldometer, Available online, <https://www.worldometers.info/coronavirus/>, 2020. accessed on 20 April.
- [8] I.T. Gbadamosi, Stay safe: helpful herbal remedies in COVID-19 infection, *Afr. J. Biomed. Res.* 23 (2020) 131–133.
- [9] I.T. Gbadamosi, Hidden Treasures of Ethnobotanical Medicine. A Faculty Lecture Delivered at the Faculty of Science, University of Ibadan on 26th June, 2019, 2019.
- [10] I. Gbadamosi, A.J.J.o.A.B. Afolayan, *in vitro* anti-radical activities of extracts of *Solanum nigrum* (L.) from South Africa, *J. App. Biosci.* 98 (2016) 9240–9251.
- [11] I. Gbadamosi, J. Moody, A.J.E.J.o.M.P. Yekini, Nutritional composition of ten ethnobotanicals used for the treatment of anaemia in Southwest Nigeria, *Eur. J. Med. Plants* 2 (2012) 140–150.
- [12] Z. Jin, X. Du, Y. Xu, Y. Deng, M. Liu, Y. Zhao, B. Zhang, X. Li, L. Zhang, C. Peng, Y. Duan, J. Yu, L. Wang, K. Yang, F. Liu, R. Jiang, X. Yang, T. You, X. Liu, X. Yang, F. Bai, H. Liu, X. Liu, L.W. Guddat, W. Xu, G. Xiao, C. Qin, Z. Shi, H. Jiang, Z. Rao, H. Yang, Structure of M(pro) from SARS-CoV-2 and discovery of its inhibitors, *Nature* 582 (2020) 289–293.
- [13] J.C. Gordon, J.B. Myers, T. Folta, V. Shoja, L.S. Heath, A. Onufriev, H++: a server for estimating pKas and adding missing hydrogens to macromolecules, *Nucleic Acids Res.* 33 (2005) W368–W371.

- [14] P.C.D. Hawkins, A.G. Skillman, G.L. Warren, B.A. Ellingson, M.T. Stahl, Conformer generation with OMEGA: algorithm and validation using high quality structures from the protein databank and cambridge structural database, *J. Chem. Inf. Model.* 50 (2010) 572–584.
- [15] OMEGA OpenEye Scientific Software, Santa Fe, NM, USA, 2013.
- [16] SZYBKI OpenEye Scientific Software, Santa Fe, 2016.
- [17] G.M. Morris, R. Huey, W. Lindstrom, M.F. Sanner, R.K. Belew, D.S. Goodsell, A. J. Olson, AutoDock4 and AutoDockTools 4: automated docking with selective receptor flexibility, *J. Comput. Chem.* 30 (2009) 2785–2791.
- [18] S. Forli, R. Huey, M.E. Pique, M.F. Sanner, D.S. Goodsell, A.J. Olson, Computational protein-ligand docking and virtual drug screening with the AutoDock suite, *Nat. Protoc.* 11 (2016) 905–919.
- [19] J. Gasteiger, M. Marsili, Iterative partial equalization of orbital electronegativity - a rapid access to atomic charges, *Tetrahedron* 36 (1980) 3219–3228.
- [20] D.A. Case, R.M. Betz, D.S. Cerutti, T.E. Cheatham, T.A. Darden, R.E. Duke, T. J. Giese, H. Gohlke, A.W. Goetz, N. Homeyer, S. Izadi, P. Janowski, J. Kaus, A. Kovalenko, T.S. Lee, S. LeGrand, P. Li, C. Lin, T. Luchko, R. Luo, B. Madej, D. Mermelstein, K.M. Merz, G. Monard, H. Nguyen, H.T. Nguyen, I. Omelyan, A. Onufriev, D.R. Roe, A. Roitberg, C. Sagui, C.L. Simmerling, W.M. Botello-Smith, J. Swails, R.C. Walker, J. Wang, R.M. Wolf, X. Wu, L. Xiao, P.A. Kollman, AMBER, University of California, San Francisco, 2016, 2016.
- [21] M.A.A. Ibrahim, K.A.A. Abdelrahman, M.F. Hegazy, In-silico drug repurposing and molecular dynamics puzzled out potential SARS-CoV-2 main protease inhibitors, *J. Biomol. Struct. Dyn.* (2020) 1–12.
- [22] M.A.A. Ibrahim, K.A.A. Abdelrahman, A.H.M. Abdelrahman, M.F. Hegazy, Natural-like products as potential SARS-CoV-2 M(pro) inhibitors: in-silico drug discovery, *J. Biomol. Struct. Dyn.* (2020) 1–13.
- [23] J. Wang, R.M. Wolf, J.W. Caldwell, P.A. Kollman, D.A. Case, Development and testing of a general amber force field, *J. Comput. Chem.* 25 (2004) 1157–1174.
- [24] J.A. Maier, C. Martinez, K. Kasavajhala, L. Wickstrom, K.E. Hauser, C. Simmerling, Improving the accuracy of protein side chain and backbone parameters from ff99SB, *J. Chem. Theor. Comput.* 11 (2015) 3696–3713, ff14SB.
- [25] C.I. Bayly, P. Cieplak, W. Cornell, P.A. Kollman, A well-behaved electrostatic potential based method using charge restraints for deriving atomic charges: the RESP model, *J. Phys. Chem.* 97 (1993) 10269–10280.
- [26] M.J. Frisch, G.W. Trucks, H.B. Schlegel, G.E. Scuseria, M.A. Robb, J.R. Cheeseman, G. Scalmani, V. Barone, B. Mennucci, G.A. Petersson, H. Nakatsuji, M. Caricato, X. Li, H.P. Hratchian, A.F. Izmaylov, J. Bloino, G. Zheng, J.L. Sonnenberg, M. Hada, M. Ehara, K. Toyota, R. Fukuda, J. Hasegawa, M. Ishida, T. Nakajima, Y. Honda, O. Kitao, H. Nakai, T. Vreven, J.A. Montgomery, J.E. Peralta, F. Ogliaro, M. Bearpark, J.J. Heyd, E. Brothers, K.N. Kudin, V.N. Staroverov, R. Kobayashi, J. Normand, K. Raghavachari, A. Rendell, J.C. Burant, S.S. Iyengar, J. Tomasi, M. Cossi, N. Rega, J.M. Millam, M. Klene, J.E. Knox, J.B. Cross, V. Bakken, C. Adamo, J. Jaramillo, R. Gomperts, R.E. Stratmann, O. Yazyev, A.J. Austin, R. Cammi, C. Pomelli, J.W. Ochterski, R.L. Martin, K. Morokuma, V.G. Zakrzewski, G.A. Voth, P. Salvador, J.J. Dannenberg, S. Dapprich, A.D. Daniels, Ö. Farkas, J. B. Foresman, J.V. Ortiz, J. Cioslowski, D.J. Fox, Gaussian 09, Gaussian inc., wallingford CT, USA, 2009.
- [27] I. Massova, P.A. Kollman, Combined molecular mechanical and continuum solvent approach (MM-PBSA/GBSA) to predict ligand binding, *Perspect. Drug Discov. Des.* 18 (2000) 113–135.
- [28] Y.H. Zhao, M.H. Abraham, J. Le, A. Hersey, C.N. Luscombe, G. Beck, B. Sherborne, I. Cooper, Rate-limited steps of human oral absorption and QSAR studies, *Pharm. Res. (N. Y.)* 19 (2002) 1446–1457.
- [29] H. Heberle, G.V. Meirelles, F.R. da Silva, G.P. Telles, R. Minghim, InteractiVenn: a web-based tool for the analysis of sets through Venn diagrams, *BMC Bioinf.* 16 (2015) 169–175.
- [30] R. Li, X. Ma, Y. Song, Y. Zhang, W. Xiong, L. Li, L. Zhou, Anti-colorectal cancer targets of resveratrol and biological molecular mechanism: Analyses of network pharmacology, human and experimental data, *J. Cell. Biochem.* 120 (2019) 11265–11273.
- [31] P. Shannon, A. Markiel, O. Ozier, N.S. Baliga, J.T. Wang, D. Ramage, N. Amin, B. Schwikowski, T. Ideker, Cytoscape: a software environment for integrated models of biomolecular interaction networks, *Genome Res.* 13 (2003) 2498–2504.
- [32] L.T. Lin, W.C. Hsu, C.C. Lin, Antiviral natural products and herbal medicines, *J. Tradit. Complement. Med.* 4 (2014) 24–35.
- [33] A. Chandwani, J. Shuter, Lopinavir/ritonavir in the treatment of HIV-1 infection: a review, *Therapeut. Clin. Risk Manag.* 4 (2008) 1023–1033.
- [34] G.A. Lee, T. Seneviratne, M.A. Noor, J.C. Lo, J.M. Schwarz, F.T. Aweeka, K. Mulligan, M. Schambelan, C. Grunfeld, The metabolic effects of lopinavir/ritonavir in HIV-negative men, *AIDS* 18 (2004) 641–649.
- [35] B. Cao, Y. Wang, D. Wen, W. Liu, J. Wang, G. Fan, L. Ruan, B. Song, Y. Cai, M. Wei, X. Li, J. Xia, N. Chen, J. Xiang, T. Yu, T. Bai, X. Xie, L. Zhang, C. Li, Y. Yuan, H. Chen, H. Li, H. Huang, S. Tu, F. Gong, Y. Liu, Y. Wei, C. Dong, F. Zhou, X. Gu, J. Xu, Z. Liu, Y. Zhang, H. Li, L. Shang, K. Wang, K. Li, X. Zhou, X. Dong, Z. Qu, S. Lu, X. Hu, S. Ruan, S. Luo, J. Wu, L. Peng, F. Cheng, L. Pan, J. Zou, C. Jia, J. Wang, X. Liu, S. Wang, X. Wu, Q. Ge, J. He, H. Zhan, F. Qiu, L. Guo, C. Huang, T. Jaki, F.G. Hayden, P.W. Horby, D. Zhang, C. Wang, A trial of lopinavir-ritonavir in adults hospitalized with severe covid-19, *new engl. J. Med.* 382 (2020) 1787–1799.
- [36] X.T. Ye, Y.L. Luo, S.C. Xia, Q.F. Sun, J.G. Ding, Y. Zhou, W. Chen, X.F. Wang, W. Zhang, W.J. Du, Z.W. Ruan, L. Hong, Clinical efficacy of lopinavir/ritonavir in the treatment of Coronavirus disease 2019, *Eur. Rev. Med. Pharmacol. Sci.* 24 (2020) 3390–3396.
- [37] T. Pansar, A. Poso, Binding affinity via docking: fact and fiction, *Molecules* 23 (2018) 1899–1909.
- [38] N.S. Pagadala, K. Syed, J. Tuszynski, Software for molecular docking: a review, *Biophys. Rev* 9 (2017) 91–102.
- [39] M. Hoffmann, H. Kleine-Weber, S. Schroeder, N. Kruger, T. Herrler, S. Erichsen, T. S. Schiergens, G. Herrler, N.H. Wu, A. Nitsche, M.A. Muller, C. Drosten, S. Pohlmann, SARS-CoV-2 cell entry depends on ACE2 and TMPRSS2 and is blocked by a clinically proven protease inhibitor, *Cell* 181 (2020) 271–280, e278.
- [40] V. Palau, M. Riera, M.J. Soler, ADAM17 inhibition may exert a protective effect on COVID-19, *Nephrol. Dial. Transplant.* 35 (2020) 1071–1072.